Supporting Information (SI)

Gas-Induced Ion-Free Stable Radical Anion Formation of Organic Semiconducting Solids as Highly Gas-Selective Probes

Seung-Heon Lee,[†,§] Byeong M. Oh,[†,§] Chan Yoo Hong,[‡] Su-Kyo Jung,[†] Sung-Ha Park,[†] Gyeong G. Jeon,[†] Young-Wan Kwon,[¶] Seokhoon Jang,[#] Youngu Lee,[#] Dongwook Kim,*[,‡] Jong H. Kim,*[,†] and O-Pil Kwon*[,†]

[†]Department of Molecular Science and Technology, Ajou University, Suwon 443-749, Korea, E-mail: opilkwon@ajou.ac.kr (O.P.K.) and jonghkim@ajou.ac.kr (J.H.K.)

[‡]Department of Chemistry, Kyonggi University, San 94-6, Iui-dong, Yeongtong-gu, Suwonsi, Gyeonggi 443-760, Korea, E-mail: dongwook-kim@kyonggi.ac.kr (D.W.K.)

[¶]KU-KIST Graduate School of Converging Science and Technology, Korea University, Seoul 136-701, Korea

[#]Department of Energy Science & Engineering, DGIST, 333, Techno JungangDaero, Hyeonpung-Myeon, Dalseong-Gun, Daegu, 42988, Korea.

[§]These authors contributed equally to this work.

A. Synthesis

NDI-based compounds were synthesized by a condensation reaction based on the literature [*Adv. Funct. Mater*., 2018, *28*, 1800346]. Meanwhile, NDI-EWG1, NDI-EWG2, NDI-EWG3, and NDI-C6 compounds have been previously reported [*Chem. Mater*. 2008, *20*, 3609; *ChemPhysChem*, 2001, *3*, 167; *Syn. Metals*, 2009, *159*, 2117], and NDI-EWG4 was newly synthesized as described below. *NDI-EWG1*: ^{1}H-NMR (400 MHz, $CDCl_3$, δ): 8.780 (s, 4H), 7.671 (d, 4H, *J* = 8.0 Hz), 7.570 (d, 4H, *J* = 8.4 Hz) 5.438 (s, 4H). *NDI-EWG2*: ^{1}H-NMR (600 MHz, $CDCl_3$, δ): 8.825 (s, 4H), 8.026 (s, 4H), 7.807 (s, 2H), 5.478 (s, 4H). *NDI-EWG3*: ^{1}H-NMR (600 MHz, $CDCl_3$, δ): 8.912 (s, 4H), 8.064 (s, 2H), 7.867 (s, 4H). *NDI-C6*: ^{1}H-NMR (400 MHz, $CDCl_3$, δ): 8.744 (s, 4H), 4.196 (t, 4H, *J* = 7.6 Hz), 1.758 (m, 4H, J = 9.2 Hz), 1.365 (m, 12H), 0.906 (t, 6H).

NDI-EWG4: 1,4,5,8-Naphthalenetetracarboxylic dianhydride (3g, 10.85 mmol) and 4-(aminomethyl)benzonitrile (3.77 g, 21.7 mmol) were dissolved in anhydrous *N,N'*-dimethylformamide (DMF, 300 mL). The solution was heated to 100 °C with stirring for 20 h and then cooled to room temperature. After removing the half of DMF solvent (150 mL), the residue was precipitated to methanol (200 mL). A light pink gray powder was obtained after drying overnight in a vacuum oven, yield = 37%, ^{1}H-NMR (600 MHz, $CDCl_3$, δ): 8.783 (s, 4H, $C_{10}H_4$), 7.632 (d, 8H, C_8H_8), 5.412 (s, 4H, C_2H_4)). Since the as-synthesized NDI-EWG4 powder has low solubility, it was purified further by sublimation. GC-MS (Agilent 5977B GC/MSD) *m/z* calcd. 496.12; found 496.3.

B. Stable Radical Anion Formation (SRAF) in Solution

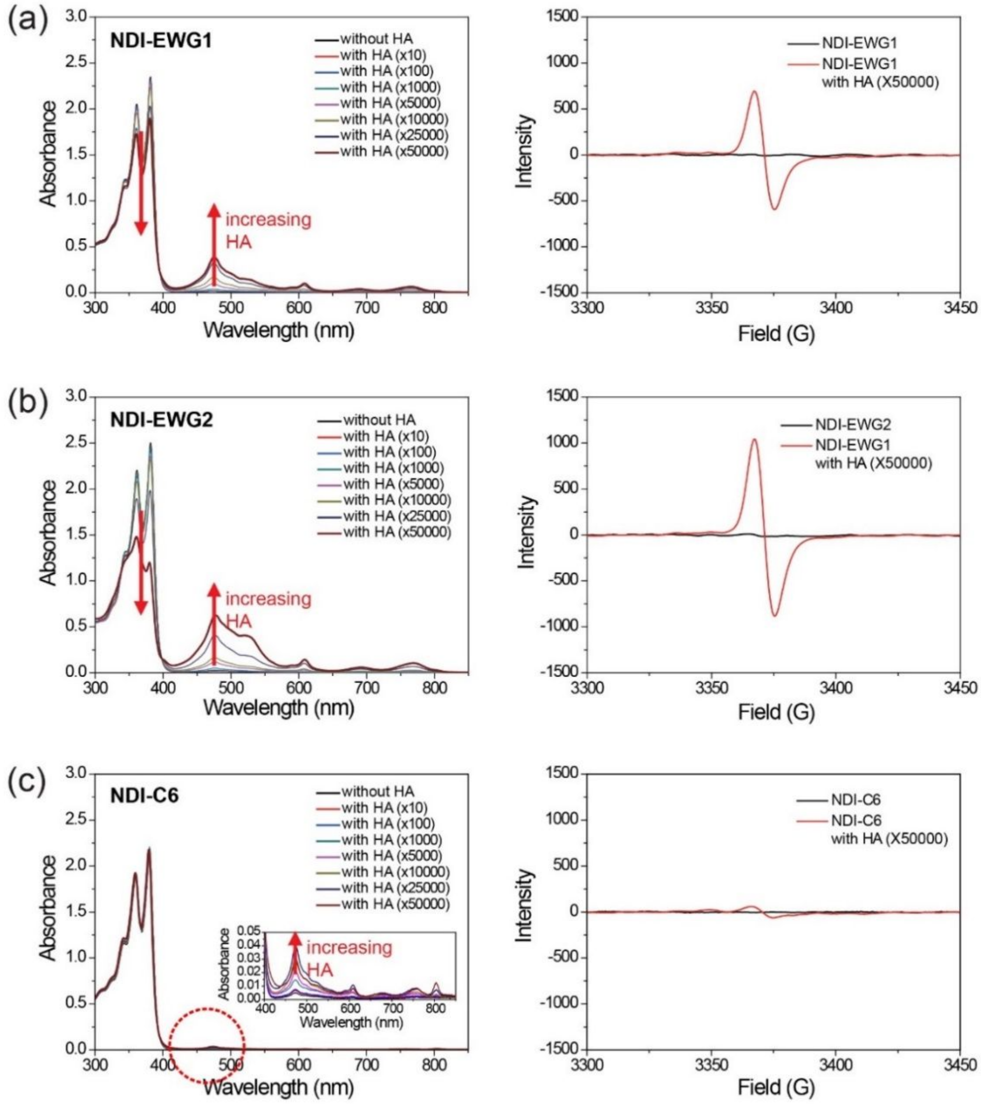

Figure S1. Absorption (left) and electron spin resonance (ESR) (right) spectra of (a) NDI-EWG1, (b) NDI-EWG2, and (c) NDI-C6 in DMF solutions (10^{-4} M) with different concentrations of a hard Lewis base: primary amine (n-hexylamine (HA)): NDI:base = 1:0, 1:10, 1:100, 1:1000, 1:5000, 1:10000, 1:25000, and 1:50000 mol/mol. UV-vis absorption spectra were measured by JASCO V-770 spectrometer and X-band continuous wave ESR spectra (JES-FA200, Jeol, Japan) of the NDI series in solution were collected at 5 mW microwave (~9.45 GHz) power with 100 kHz field modulation (10 G modulation amplitude) at room temperature.

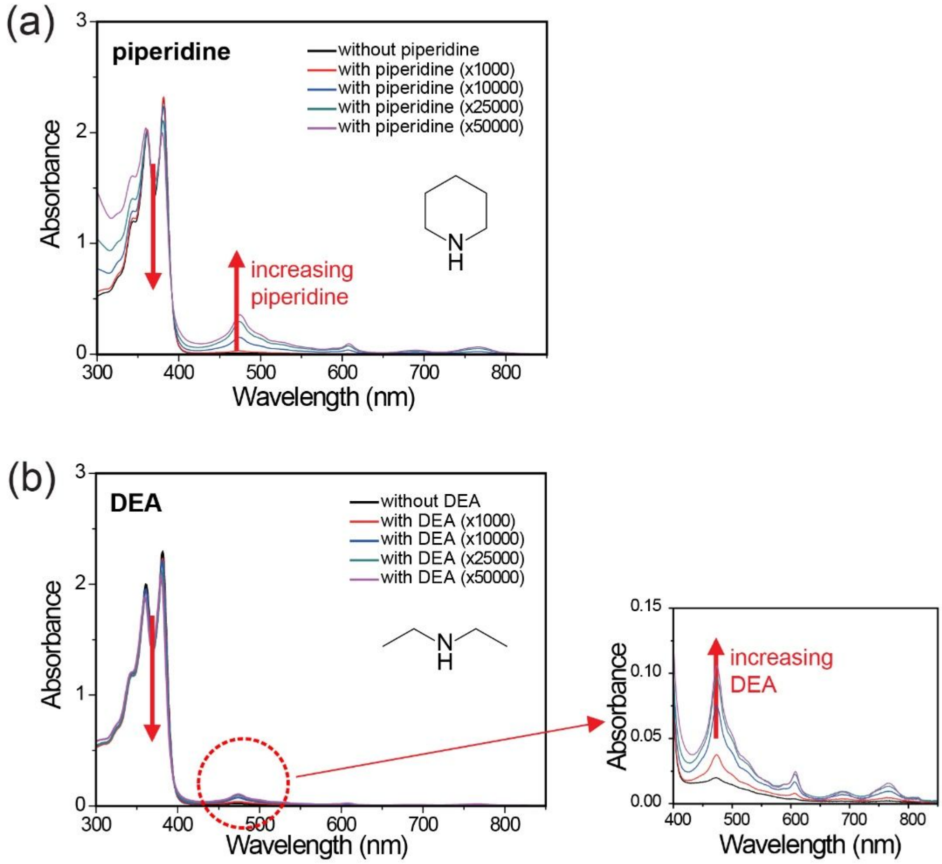

Figure S2. Absorption spectra of NDI-EWG1 in DMF (10^{-4} M) with hard Lewis bases: secondary amines ((a) piperidine and (b) diethylamine (DEA)): NDI:base = 1:0, 1:1000, 1:10000, 1:25000, and 1:50000 mol/mol.

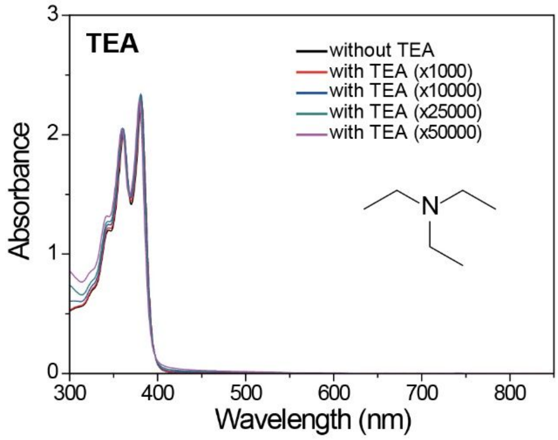

Figure S3. Absorption spectra of NDI-EWG1 in DMF solutions (10^{-4} M) with a borderline Lewis base: tertiary amine (triethylamine (TEA)): NDI:base = 1:0, 1:1000, 1:10000, 1:25000, and 1:50000 mol/mol.

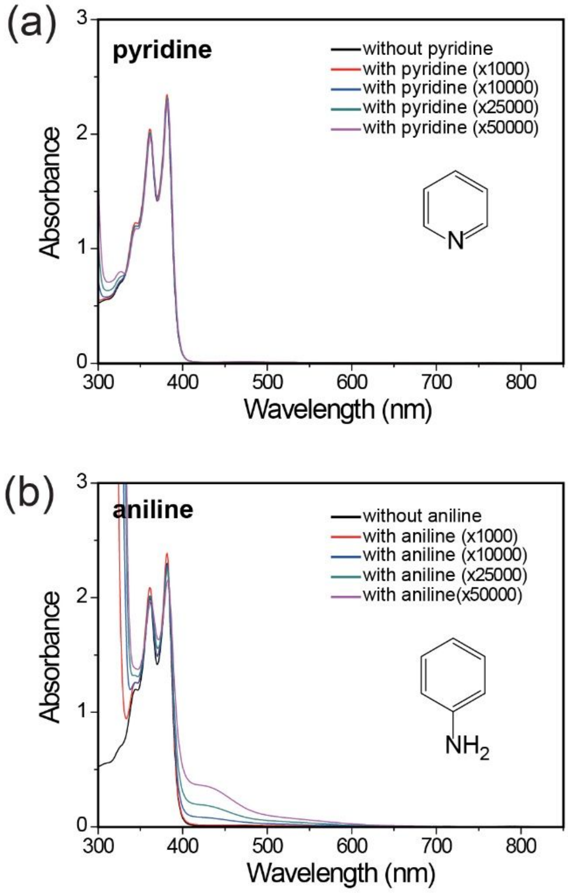

Figure S4. Absorption spectra of NDI-EWG1 in DMF solutions (10^{-4} M) with borderline Lewis bases: aromatic (a) heterocyclic pyridine and (b) non-heterocyclic aniline (NDI:base = 1:0, 1:1000, 1:10000, 1:25000, and 1:50000 mol/mol). Note that NDI-EWG1 does not form a radical anion with aromatic amines. In Figure S4b, the increase in the absorption of the NDI-EWG1 solution in the range of 400–600 nm with increasing aniline concentration originates from law material (aniline) absorption.

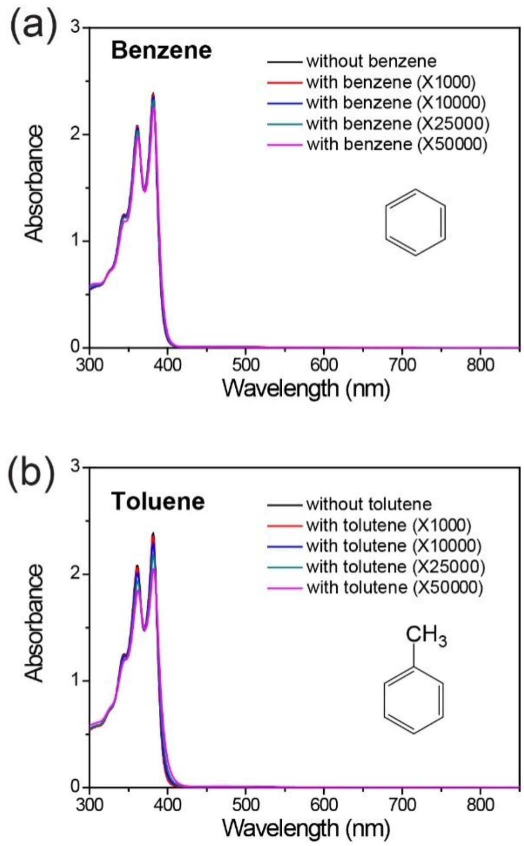

Figure S5. Absorption spectra of NDI-EWG1 in DMF solutions (10^{-4} M) with soft Lewis bases: non-polar aromatic (a) benzene and (b) toluene (NDI:base = 1:0, 1:1000, 1:10000, 1:25000, and 1:50000 mol/mol). Note that NDI-EWG1 does not form a radical anion with non-polar aromatic compounds.

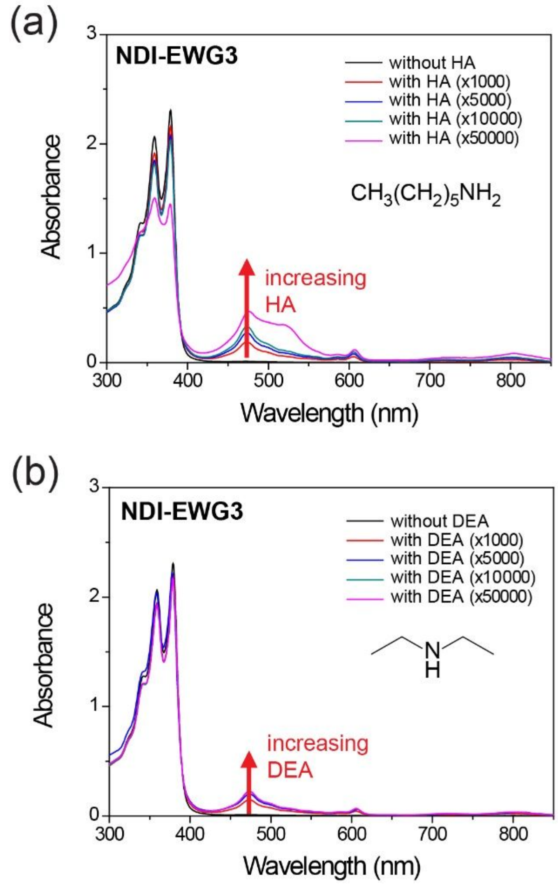

Figure S6. Absorption spectra of NDI-EWG3 in DMF solutions (10^{-4} M) with hard Lewis bases: (a) n-hexylamine (HA) and (b) diethylamine (DEA): NDI:base = 1:0, 1:1000, 1:5000, 1:10000, and 1:50000 mol/mol.

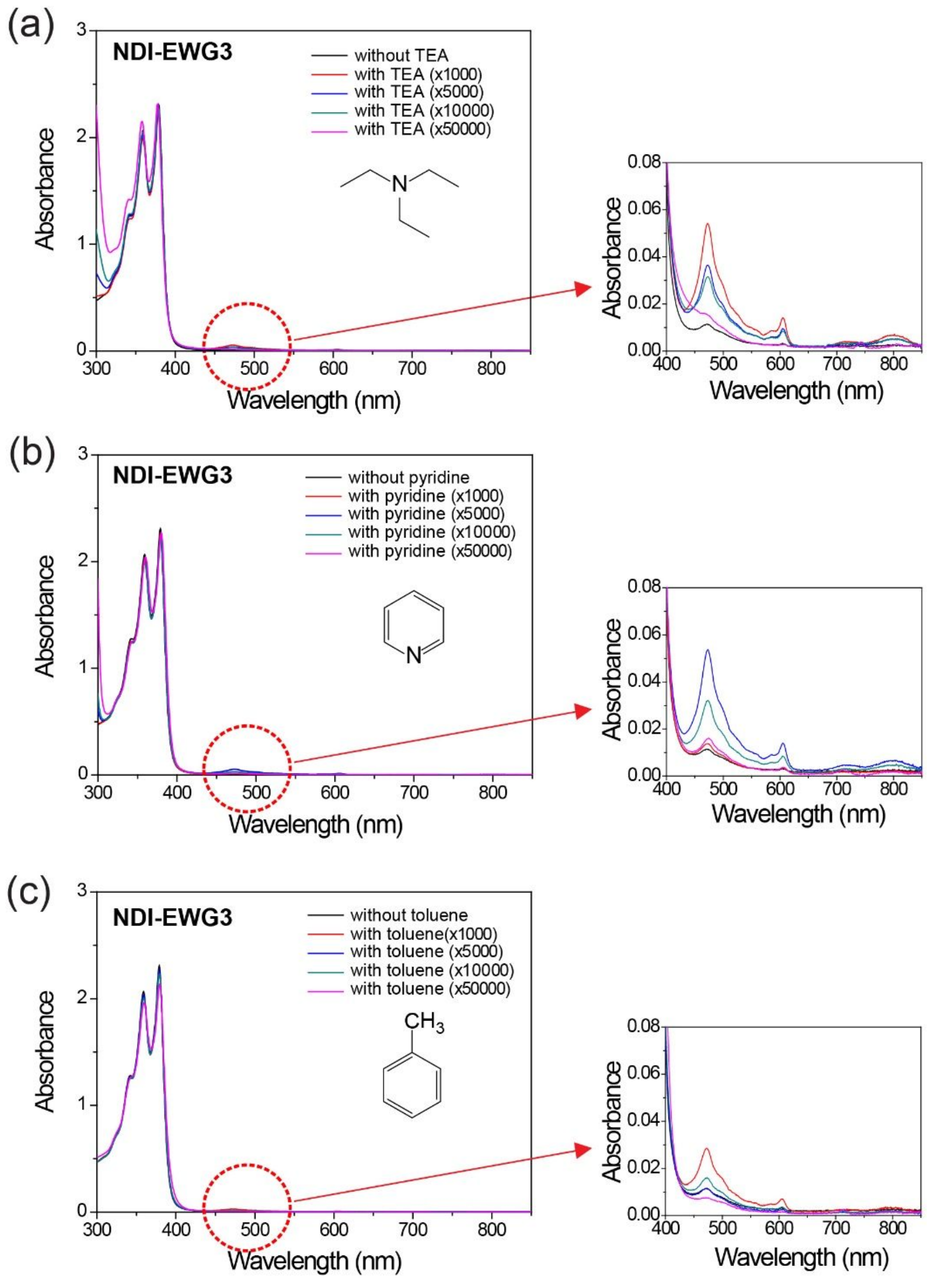

Figure S7. Absorption spectra of NDI-EWG3 in DMF solutions (10^{-4} M) with borderline Lewis bases: (a) triethylamine (TEA), (b) pyridine, and soft Lewis base (c) non-polar aromatic toluene; NDI:base = 1:0, 1:1000, 1:5000, 1:10000, and 1:50000 mol/mol. NDI-EWG3 exhibits clear SRAF behavior at low concentrations of borderline and soft bases (e.g., 1:1000 for TEA and toluene, and 1:5000 for pyridine). In contrast, at high concentrations of the bases in solution, the tendency of radical anion formation decreases unexpectedly, which may be attributed to the side effect at high concentrations (e.g., strong intermolecular interactions).

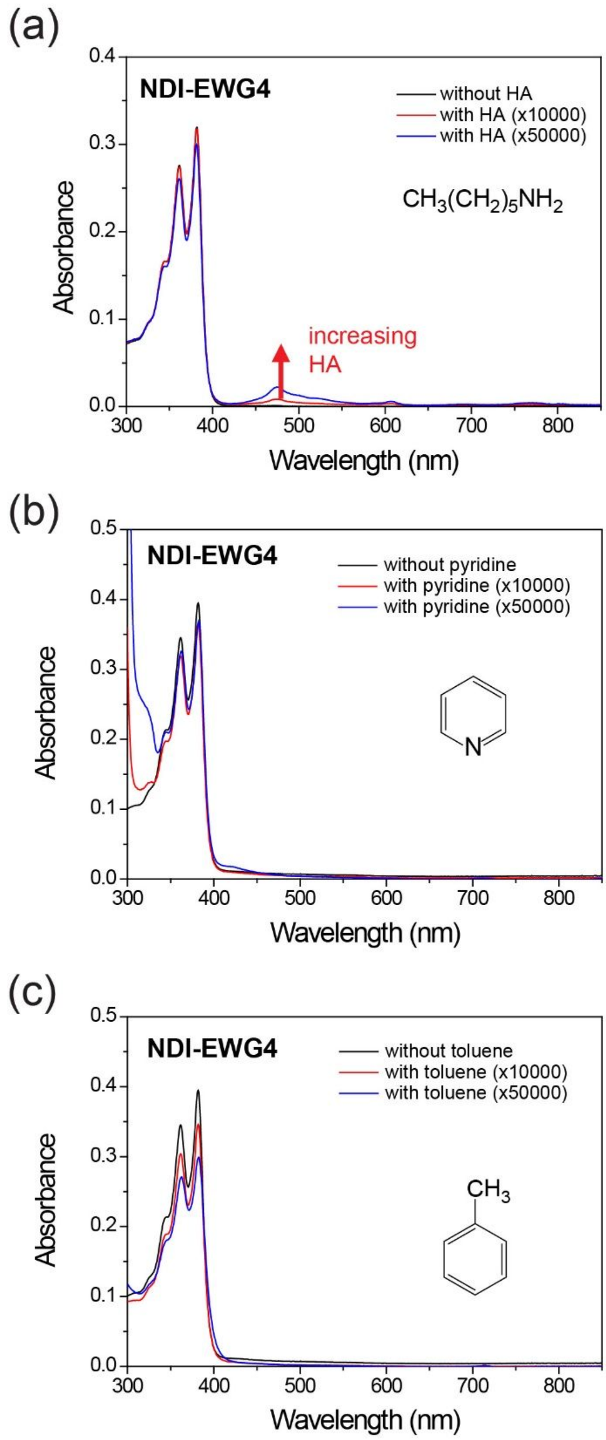

Figure S8. Absorption spectra of NDI-EWG4 in DMF solution (10^{-5} M) with different concentrations of (a) hard Lewis base (n-hexylamine (HA)), (b) borderline Lewis base (pyridine), and (c) soft Lewis base (toluene): NDI:base = 1:0, 1:10000, and 1:50000 mol/mol.

C. NDI-EWG1 Crystals

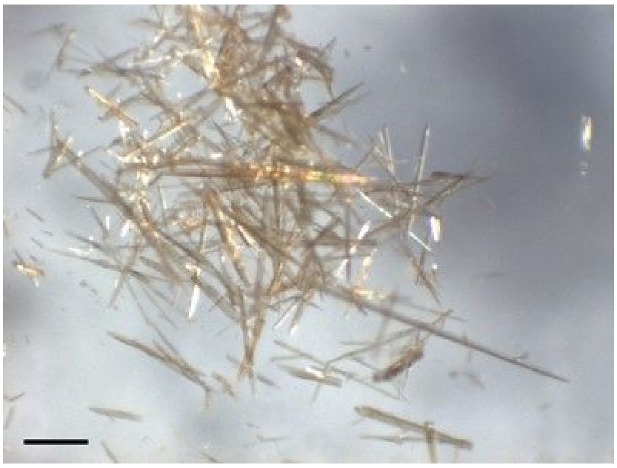

Figure S9. Photographs of as-grown NDI-EWG1 crystals from a DMF solution (scale bar: 200 μm)

D. OFET-Based Gas Sensors

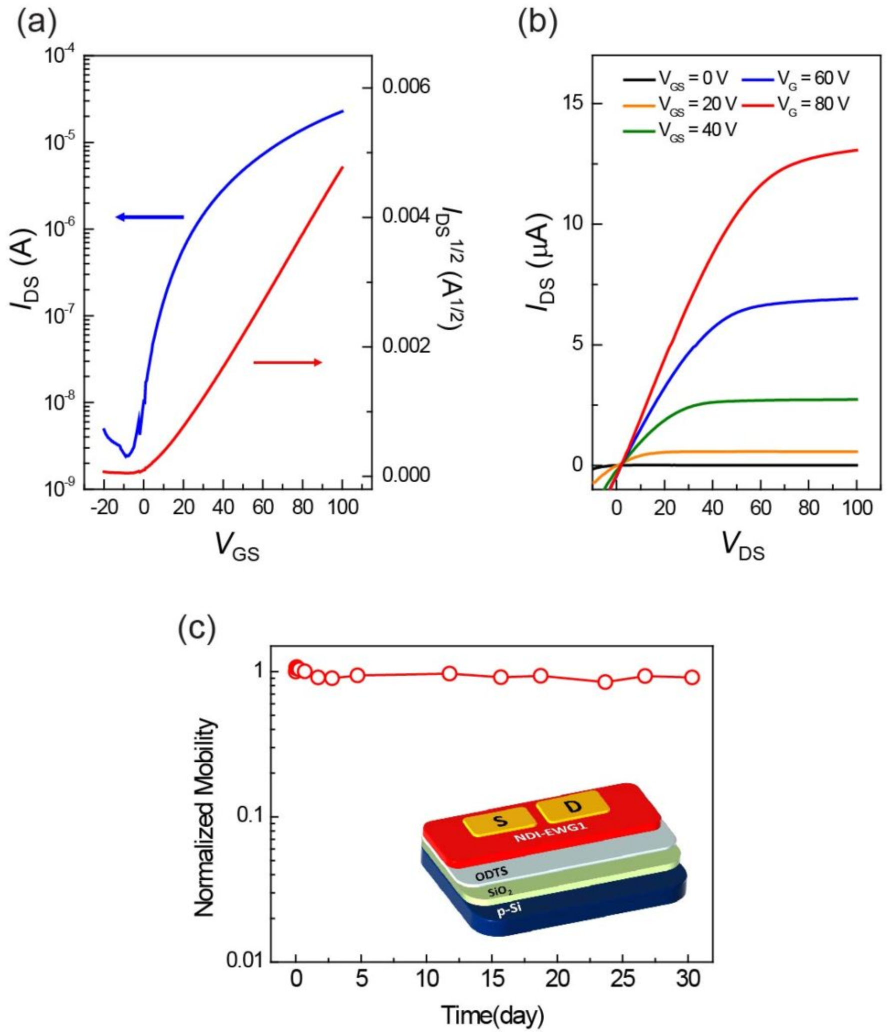

Figure S10. (a) Transfer, (b) output curves, and (c) air stability measurements for film-type NDI-EWG1-based OFET (inset: schematic of the fabricated OFET device structure).

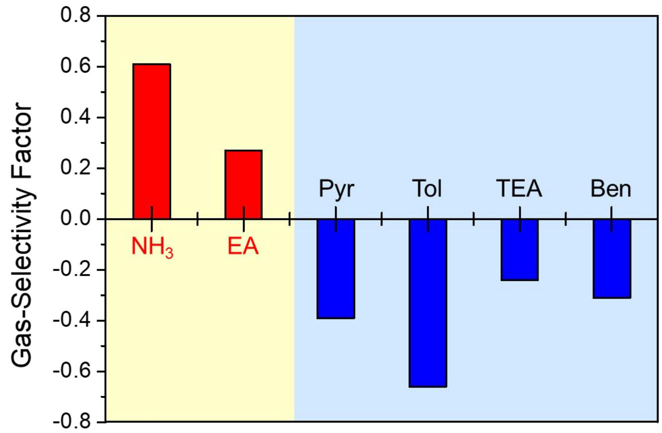

Figure S11. Gas-selective factors for different types of gases.

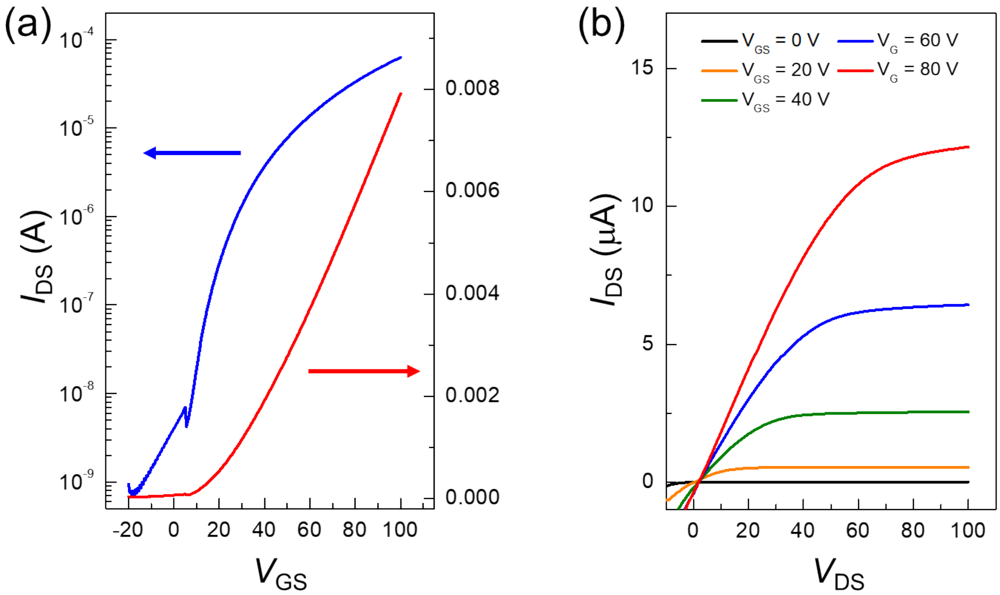

Figure S12. (a) Transfer and (b) output curves for fibrillar-type NDI-EWG1-based OFET.

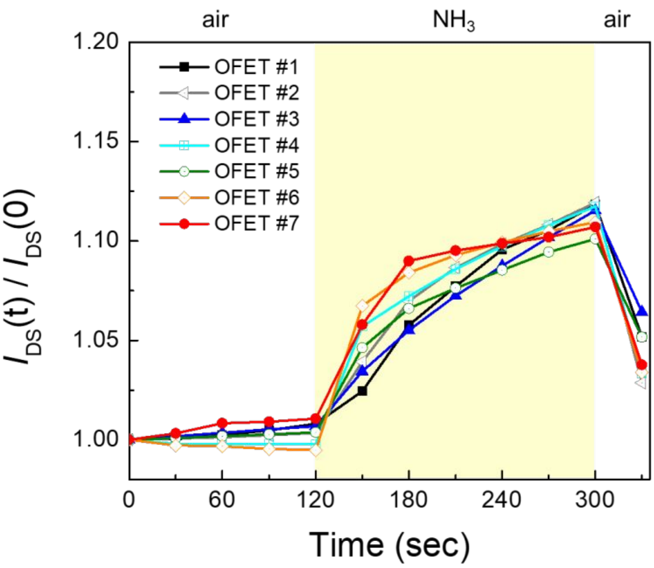

Figure S13. The reproducibility of the responsivity for the first cycle sensing measurement of NDI-EWG1-based OFETs.